# Helicopter Gas Turbine Engine Performance Analysis
# A Multivariable Approach

Arush, Ilan; Pavel, Marilena

**DOI**
10.1177/0954410017741329

**Publication date**
2017

**Document Version**
Accepted author manuscript

**Published in**
Institution of Mechanical Engineers. Proceedings. Part G: Journal of Aerospace Engineering

# Helicopter Gas Turbine Engine Performance Analysis - A Multivariable Approach

Ilan Arush[1]
*National Test Pilot School, Mojave, California, 93502. Email: iarush@ntps.edu*

Marilena D. Pavel[2]
*Faculty of Aerospace Engineering, Delft University of Technology, Delft, The Netherlands*

**Helicopter performance relies heavily on the available output power of the engine(s) installed. A simplistic single-variable analysis approach is often used within the flight-testing community to reduce raw flight-test data in order to predict the available output power under different atmospheric conditions. This simplistic analysis approach often results in unrealistic predictions. This paper proposes a novel method for analyzing flight-test data of a helicopter gas turbine engine. The so-called "Multivariable Polynomial Optimization under Constraints" (MPOC) method is capable of providing an improved estimation of engine performance and maximum available power. The MPOC method relies on optimization of a multivariable polynomial model subjected to equalities and inequalities constraints. The Karush-Khun-Tucker (KKT) optimization method is used with the engine operation limitations serving as inequalities constraints. The proposed MPOC method is applied to a set of flight-test data of a Rolls Royce/Allison MTU250-C20 gas turbine engine, installed on a MBB BO-105M helicopter. It is shown that the MPOC method can predict the engine output power under a wider range of atmospheric conditions and that the standard deviation of the output power estimation error is reduced from 13hp in the current single-variable method to only 4.3hp using the MPOC method (over 300% improvement).**

## Nomenclature

$A$ = Matrix containing numerical regressors

$\alpha_j^i$ = generic multivariable polynomial coefficient

$Ng$ = engine compressor speed

[1] Corresponding Author. Chief Theoretical Knowledge Instructor and Chief RW Academics, National Test Pilot School, Mojave, California.
[2] Assistant Professor, Control and Simulation, Faculty of Aerospace Engineering, Delft University of Technology, Kluyverweg, 2629HS Delft, The Netherlands, AIAA Member.

$TGT$ = engine temperature (Turbine Gas Temperature)

$SHP$ = engine output power (Shaft Horse Power)

$W_f$ = engine fuel-flow

$CN_g \triangleq \frac{N_g}{\sqrt{\theta}}$ = corrected engine compressor speed

$CTGT \triangleq \frac{TGT}{\theta}$ = corrected engine temperature (Turbine Gas Temperature)

$CSHP \triangleq \frac{SHP}{\delta\sqrt{\theta}}$ = corrected engine output power (Shaft Horse Power)

$CW_f \triangleq \frac{W_f}{\delta\sqrt{\theta}}$ = corrected engine fuel-flow

$\delta$ = relative static air pressure

$\theta$ = relative static air temperature

$\vec{E}_r$ = engine output power estimation error vector

$a_i, b_i, c_i$ = generic single-variable polynomial coefficients

$\vec{b}$ = column vector to represent experimental CSHP

$f$ = generic multivariable function in $x_i$ to be maximized

$g_j$ = inequality constraints

$h_k$ = equality constraints, multivariable function in $x_i$

$\lambda_i$ = Lagrange multipliers associated with equality constraints

$\mu_i$ = Lagrange multipliers associated with inequality constraints

$i, j$ = indices

$x_i$ = variables of a generic multivariable function

## I. Introduction

FLIGHT testing is an expensive activity that requires efficient methods for predicting correctly the helicopter performance. Such methods involve considerations regarding testing techniques and data reduction of the raw flight-test data. The present paper relates to the helicopter maximum engine power testing methodology. In the current method the flight-test data are analyzed based on single-variable models. The paper proposes a novel method involving multivariable polynomials defined for the engine parameters, i.e. Shaft Output Power, Compressor speed, Temperature

and Fuel-Flow. It will be shown that such an approach can result in more realistic predictions. The paper is structured as follows: after a short introduction, section II gives the current methodology for flight-test data analysis w.r.t. maximum engine power. In section III a novel methodology is defined and demonstrated involving multivariable regression analysis for maximum engine power. Final conclusions and recommendations complete the paper.

## II. Single-variable Analysis Method

The useful performance of any helicopter depends on the amount by which the power available exceed the power required [Ref. 1]. The current method widely used within flight-test community for determining the maximum output power of the helicopter engine based on flight-test data for consists on recording stabilized engine(s) parameters (such as temperature, compressor speed, fuel-flow and shaft output power) accompanied by their corresponding atmospheric conditions prevailed during the test [Ref. 2]. These flight-test data are gathered while flying the helicopter throughout its certified envelope and collecting engine parameters to their approved operating limitations. Once a substantial data base is gathered it can be analyzed with the final goal of deriving the maximum shaft output power that the turbine engine can deliver under various combinations of atmospheric conditions. One should remember that the limiting factor for the maximum output power could change under different atmospheric conditions (for example, under hot day conditions the engine maximum output power could be limited by the engine temperature while under relatively cold day conditions the maximum engine compressor speed could limit the maximum power the engine can deliver. The flight-test data analysis must "decide" on both what the maximum power is and which its associated limiting factor is. Usual limiting factors are the engine temperature, the engine compressor speed or the fuel flow to the engine. An additional limiting factor that often comes into play is maximum transmission torque. This limitation is not an engine limitation as such (it is more the platform limitation) but it can have a fundamental effect on maximum output power of the engine. This entire process described is often referred to as "the analysis to define the installed engine available power".

Dimensional analysis concepts are intensively used in performance flight-testing. Applying non-dimensional analysis tools allow the flight-test team to reduce the number of dimensional parameters involved in the physical problem, and hence to reduce substantially the number of flight-test sorties required, saving time and resources [Ref. 3]. The first step in analyzing the engine data is therefore not surprisingly related to correcting or non-dimensionalizing the raw flight-test data. There are mainly four engine parameters, i.e. Shaft Output Power,

Compressor speed, Temperature and Fuel-Flow which are corrected using the corresponding atmospheric conditions and are converted into, CSHP, CNg, CTGT & $CW_f$ respectively. The mathematical process of non-dimensionalizing the gas turbine engine parameters is based on the Buckingham PI Theorem [Ref. 4].

Next step will concentrate on applying common methods of linear regression in order to best fit three ***separate single-variable*** polynomials as given by Eq. (1) to (3). These polynomials give the correlation between the experimental data; the mathematical relation between the corrected engine power and each of the other corrected engine parameters. They are usually of 3rd order so that they can capture an inflection point representing an important physical characteristic of the engine.

$$CSHP = f_1\left(CN_g\right) \approx b_0 + \sum_{i=1}^{n} b_i \left(CN_g\right)^i \therefore n = 3 \tag{1}$$

$$CSHP = f_2\left(CTGT\right) \approx a_0 + \sum_{i=1}^{n} a_i \left(CTGT\right)^i \therefore n = 3 \tag{2}$$

$$CSHP = f_3\left(CW_f\right) \approx c_0 + \sum_{i=1}^{n} c_i \left(CW_f\right)^i \therefore n = 3 \tag{3}$$

Each single-variable polynomial can then be treated like a 'finger print' of the installed engine in the particular helicopter type and represents the mathematical relationship between the corrected output power and the separate corrected engine parameter (engine temperature, engine compressor speed or engine fuel-flow).

As example throughout this paper consider the flight-test data gathered for a Rolls Royce/Allison MTU250-C20 gas turbine engine installed as the left engine on a MBB BO-105M helicopter used for training at the National Test Pilot School in Mojave, California. Applying Eq. (1) to (3) to this set of flight-test data and using least-squares technique results in Eq. (4) to (6). Figure 1 presents the three non-dimensional engine parameters plots for the example flight-test data.

The last step in this analysis method is to evaluate the maximum available output power (in physical units) the engine is capable of delivering under a wide range of atmospheric conditions. For an atmospheric condition of choice, the engine output power is calculated separately in each path; the path of compressor speed limited engine (substituting the engine compressor speed limitation in Eq. (1) , the path of temperature limited engine (substituting the engine maximum allowable temperature limitation in Eq. (2)) and the path of fuel flow limited engine (substituting the engine fuel flow limitation in Eq. (3)). The three calculated values for the engine output power are then compared, first amongst themselves and then against the maximum transmission torque (transmission limitation). The maximum available power of the engine will be assessed as the *minimum* out of all 4 channels [Ref. 5].

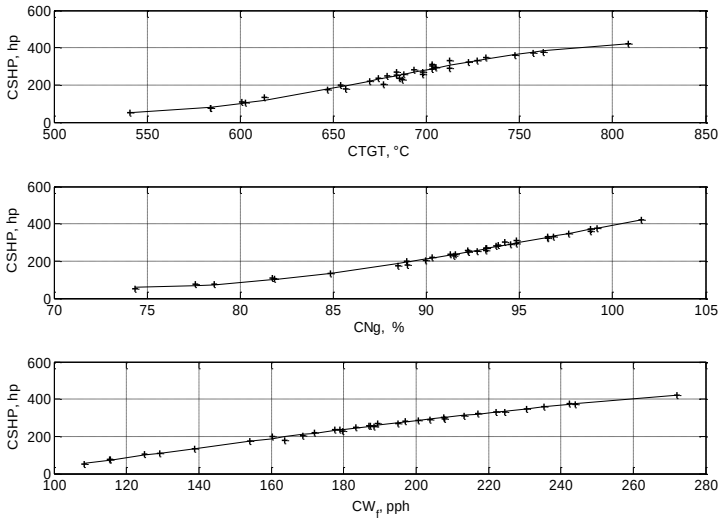


**Figure 1.** Non-Dimensional Single-Variable Engine Performance. *Data represents 34 stabilized engine operation points during flight at various conditions. The corrected engine output power (CSHP) is separately presented against each of the engine corrected parameters, corrected engine temperature, corrected compressor speed and corrected engine fuel flow (fuel weight flow).*

$$CSHP = \tilde{f}_1\left(CN_g\right) = -0.009947\left(CN_g\right)^3 + 2.9534\left(CN_g\right)^2 - 273.47\left(CN_g\right) + 8153.2 \tag{4}$$

$$CSHP = f_2\left(CTGT\right) = -3.328\times10^{-5}\left(CTGT\right)^3 + 0.0677\left(CTGT\right)^2 - 43.87\left(CTGT\right) + 9256.7 \tag{5}$$

$$CSHP = f_3\left(CW_f\right) = -9.3718\times10^{-6}\left(CW_f\right)^3 + 0.0020359\left(CW_f\right)^2 + 2.5551\left(CW_f\right) - 234.32 \tag{6}$$

The data presented in Fig. 2 were derived by following the described procedure with the example polynomials (Eq. 4, 5, 6). Figure 2 shows the analyzed data for up to 12,000 ft. of pressure-altitude and for five distinct day conditions; a standard day (ISA), 10°C and 20°C hotter than standard, 5°C and 10°C colder than standard day

conditions. Figure 2 presents the *estimated* maximum continuous output power of the engine based on this set of flight-test data.

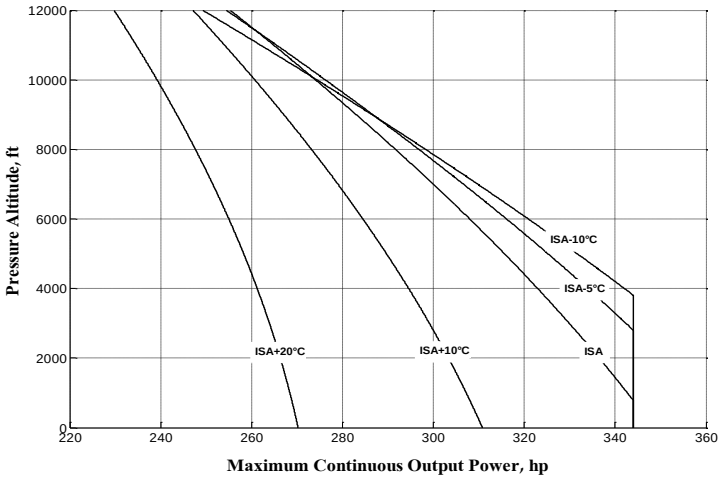


**Figure 2**. Estimated maximum continuous power of the example engine. *Note the engine as installed in the helicopter is transmission limited for ISA, ISA-5 and ISA-10 conditions.*

The continuous power rating of this type of engine was set at engine temperature of 738°C and compressor speed of 105%. For the fuel-flow a fictitious limitation (@ 450 pounds per hour) was used (since, for this specific engine and under atmospheric conditions used, this parameter of the engine is never a limiting factor). Another limitation mentioned above is the transmission limitation. This was at 344 hp for the continuous rating. It can be easily seen from Fig. 2 that for ISA, ISA-5 and ISA-10 day conditions the helicopter maximum power is transmission limited from sea level up to 790 ft., 2800 ft. and 3800 ft. above sea level correspondingly. For higher pressure-altitudes the engine becomes temperature limited. As for a 10°C and 20°C hotter than standard day, analysis suggests the engine output power is temperature limited from sea level and above.

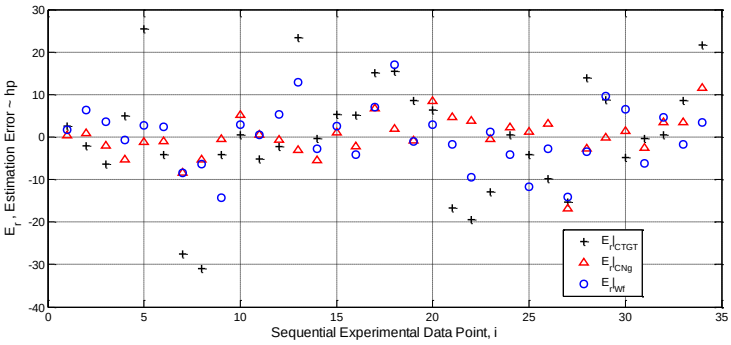


**Figure 3.** Engine output power estimation errors using single variable models. *Note the relative large estimation errors of up to 30 hp using the engine temperature variable.*

The major disadvantage of this analysis method lies in the intrinsic assumption of independency between the rules of operation in all three engine limiting factors. This disadvantage manifest itself by the unrealistic behavior of the three lines of ISA, ISA-5°C and ISA-10°C crossing each other above pressure-altitude of 8000 ft as seen in Fig. 2. It is physically impossible for a temperature limited engine to deliver more power whilst the ambient

temperature is higher. The absolute errors between actual measured engine output power and the corresponding predicted values using the reduced polynomials (Eq. 4, 5, 6) are calculated using Eq. 7, 8 & 9 and presented in Fig. 3.

These errors were found to be normally distributed about a practically zero mean. Figure 4 shows the error standard deviation for each prediction channel plotted against its relevant error mean. This figure also includes a horizontal bar to represent the 95% confidence level interval range for the mean of the error. This bar shows where the mean of the error can be found for 95% confidence level. Looking at this figure one can see that the output power based on engine temperature (Eq. 4) presents the worst performance; the relevant standard deviation of this error is 13hp and under 95% confidence level the mean of the estimation could be found anywhere along a range of ±4.6hp. A standard deviation of 13hp is considered a substantial error value for power predictions.

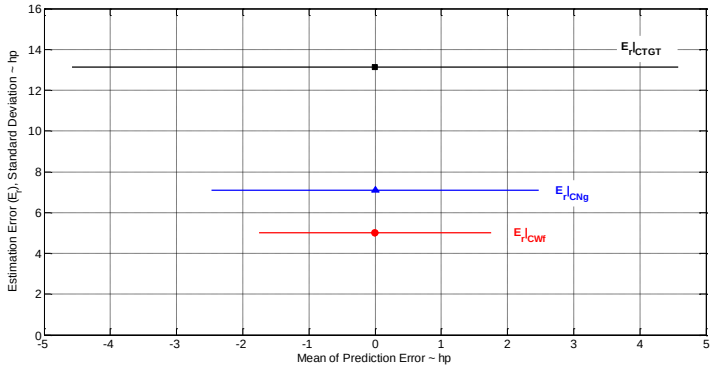


**Figure 4.** The mean and standard deviation of the single variable estimation errors. *The engine temperature based estimation presented the worst performance with an error standard deviation of 13hp.*

$$\vec{E}_r\big|_{CNg} = \left\{CSHP_i - f_1\left(CNg_i\right)\right\} \therefore i = 1,\ldots 34 \tag{7}$$

$$\vec{E}_r\big|_{CTGT} = \left\{CSHP_i - f_2\left(CTGT_i\right)\right\} \therefore i = 1,\ldots 34 \tag{8}$$

$$\vec{E}_r\big|_{W_f} = \left\{CSHP_i - f_3\left(W_{fi}\right)\right\} \therefore i = 1,\ldots 34 \tag{9}$$

Concluding, the current method used for determining the maximum output power of the helicopter engine can result in large errors and unrealistic predictions. Next chapter will propose a new method to improve flight-test data analysis.

## III. Proposed Multivariable Analysis Method

In the following sections a novel analysis method referred to as 'Multivariable Polynomial Optimization under Constraints' (MPOC) is proposed. This method requires no change to the way engine performance flight-test sorties are carried out. Using the elegant method of *projection onto subspaces* a list of mathematical candidate models will be derived to best represent the relationship between the engine output power and the engine parameters. The maximum engine output power will be assessed as an optimization problem under constraints. Since our problem has both equalities and inequalities constraints, the Karush-Khun-Tucker (KKT) method which deals with both type of constraints will be utilized.

The proposed method presented in this chapter will be exemplified with the same flight-test data used in the previous chapter dealing with the current analysis method.

### A. Multivariable Linear Regression

A *convenient* mathematical relationship needs to be found for representing the flight-test data. Polynomials serve great role in flight-testing due to their simplicity which makes them suitable candidates for best-fit type models. Different math model search algorithm were developed in the literature of specialty for optimizing regression models of multivariate experimental data obtained in aviation. For examples see [Ref. 6, 7, 8]

The MPOC method seeks for a *multivariable* polynomial limited to the third order as in the current method. This section presents the process of finding a best-fit third order multivariable polynomial to relate between the corrected shaft output power, the corrected compressor speed, corrected engine temperature and corrected fuel flow to the engine. For simplification and based on common practice, six basic two-variable polynomials of the third order are defined using the three independent engine variables. This results in six different combinations as presented in Table 1. It can be seen from Table 1 that each mathematical term yields six lower order terms resulting in a long list of 42 regressors. However, many of the lower order terms are merely duplicates and can be dismissed. Filtering out repeating terms gives an updated list of regressors as presented in Table 2. This table corresponds to a list of 18 candidate regressors to work with for a best fit mathematical expression under the generic expression as given by Eq. 10.

**Table 1**: List of 3rd order polynomials and their lower order terms

| # | Mathematical Term | List of Lower Order Terms |
|---|---|---|
| 1 | $(CN_g)^3(CTGT)$ | $CN_g; (CN_g)^2; (CN_g)^3; CTGT; (CTGT)(CN_g); (CTGT)(CN_g)^2$ |
| 2 | $(CN_g)^3(CW_f)$ | $CN_g; (CN_g)^2; (CN_g)^3; CW_f; (CW_f)(CN_g); (CW_f)(CN_g)^2$ |
| 3 | $(CTGT)^3(CN_g)$ | $CTGT; (CTGT)^2; (CTGT)^3; CN_g; (CN_g)(CTGT); (CN_g)(CTGT)^2$ |
| 4 | $(CTGT)^3(CW_f)$ | $CTGT; (CTGT)^2; (CTGT)^3; CW_f; (CW_f)(CTGT); (CW_f)(CTGT)^2$ |
| 5 | $(CW_f)^3(CN_g)$ | $CW_f; (CW_f)^2; (CW_f)^3; CN_g; (CN_g)(CW_f); (CN_g)(Cw_f)^2$ |
| 6 | $(CW_f)^3(CTGT)$ | $CW_f; (CW_f)^2; (CW_f)^3; CTGT; (CTGT)(CW_f); (CTGT)(Cw_f)^2$ |

$$CSHP = f\left(CNg, CTGT, CW_f\right) \approx \alpha_0 + \sum_{i=1}^{n}\left\{\alpha_i f_i\left(CNg, CTGT, CW_f\right)\right\} \therefore n = 18 \tag{10}$$

**Table 2**: Updated list of regressors for best fit hierarchical math regression model

| | | | | | |
|---|---|---|---|---|---|
| $f_1 = (CN_g)^3$ | $f_4 = (CTGT)^3$ | $f_7 = (CW_f)^3$ | $f_{10} = (CN_g)(CTGT)$ | $f_{13} = (CN_g)^2(CTGT)$ | $f_{16} = (CN_g)(CTGT)^2$ |
| $f_2 = (CN_g)^2$ | $f_5 = (CTGT)^2$ | $f_8 = (CW_f)^2$ | $f_{11} = (CN_g)(CW_f)$ | $f_{14} = (CN_g)^2(CW_f)$ | $f_{17} = (CN_g)(CW_f)^2$ |
| $f_3 = CN_g$ | $f_6 = CTGT$ | $f_9 = CW_f$ | $f_{12} = (CTGT)(CW_f)$ | $f_{15} = (CTGT)^2(CW_f)$ | $f_{18} = (CTGT)(CW_f)^2$ |

With the 18 derived regressors one has an enormous amount of possible models to check. The case can be thought as a combination of 1,2,3,…,18 functions from a set of 18 regressors, i.e. 262,143 possibilities as per Eq. 11.

$$N = \binom{18}{1} + \binom{18}{2} + \ldots + \binom{18}{18} = \frac{18!}{1!17!} + \frac{18!}{2!16!} + \ldots + \frac{18!}{0!18!} = 262{,}143 \tag{11}$$

The number of possible combinations can be reduced by setting a base model which is a linear combination of the elementary regressors $f_1$ to $f_9$ (Eq. 13). The polynomial as given by Eq. 13 is addressed in this paper as *Model number 1*. This way, the problem has been reduced to finding a model which will be constructed from Model 1

superimposed with any combination of the regressors $f_{10}$ to $f_{18}$. The number of combinations is now reduces to 512 as per Eq. 12.

$$N' = 1 + \binom{9}{1} + \binom{9}{2} + \ldots + \binom{9}{9} = 1 + \frac{9!}{1!8!} + \frac{9!}{2!7!} + \ldots + \frac{9!}{0!9!} = 512 \tag{12}$$

This still represents a lot of combinations but more manageable as number. Within the limited scope of this paper a performance comparison between 10 different models from the 512 is presented. Model 1 presented as Eq. 13 is simply being added with the 9 regressors ($f_{10}$ to $f_{18}$ ,of Table 2), one at a time. This process of providing candidate multivariable polynomials is presented mathematically as Eq. 14. Equation 15 presents the suggested model number 4 ($CSHP_{M4}$) as a particular case of the generic formula described by Eq. 14.

$$\begin{aligned} CSHP_{M1} = {} & \alpha_1^1 \left(CN_g\right)^3 + \alpha_2^1 \left(CN_g\right)^2 + \alpha_3^1 \left(CN_g\right) + \alpha_4^1 \left(CTGT\right)^3 + \alpha_5^1 \left(CTGT\right)^2 + \alpha_6^1 \left(CTGT\right) + \\ & + \alpha_7^1 \left(CW_f\right)^3 + \alpha_8^1 \left(CW_f\right)^2 + \alpha_9^1 \left(CW_f\right) + \alpha_0^1 \qquad \textit{Model number } 1 \end{aligned} \tag{13}$$

$$CSHP_{MK} = \sum_{i=0}^{9} \alpha_i^K f_i\left(CN_g, CTGT, CW_f\right) + \sum_{j=10}^{K+8} \alpha_j^K f_j\left(CN_g, CTGT, CW_f\right) \therefore \left\{ f_0 \triangleq 1, K = 1, 2, \ldots, 10 \right\} \tag{14}$$

$$\begin{aligned} CSHP_{M4} = {} & \alpha_1^4 \left(CN_g\right)^3 + \alpha_2^4 \left(CN_g\right)^2 + \alpha_3^4 \left(CN_g\right) + \alpha_4^4 \left(CTGT\right)^3 + \alpha_5^4 \left(CTGT\right)^2 + \alpha_6^4 \left(CTGT\right) + \\ & + \alpha_7^4 \left(CW_f\right)^3 + \alpha_8^4 \left(CW_f\right)^2 + \alpha_9^4 \left(CW_f\right) + \alpha_{10}^4 \left(CN_g\right)\left(CTGT\right) + \alpha_{11}^4 \left(CN_g\right)\left(CW_f\right) + \\ & + \alpha_{12}^4 \left(CTGT\right)\left(CW_f\right) + \alpha_0^4 \end{aligned} \tag{15}$$

**B. Fitting the Suggested Models with Experimental Data**

This section presents the method used to fit the 10 proposed multivariable models (Eq. 14, for M=1 to 10) with actual experimental flight-test data. The method used is based on a linear Algebra concept known as *projection onto subspaces* [Ref. 9].

1) Experimental Data Fitting to Model number 1.

The 34 flight-test data points of the example engine considered in this paper are next substituted in Eq. 13. This gives a linear system of 34 equations with 10 unknowns (the coefficients $\alpha_n^1$). This set of equations is compactly represented as Eq. 16. The matrix A is of size of (34x10) and contains the numerical regressors as columns, α is a

column vector (34x1) containing the unknown coefficients and b is a column vector (34x1) representing the measured experimental corrected output power of the engine (CSHP).

$$\left[A\right]\cdot\vec{\alpha}=\vec{b} \tag{16}$$

Substituting the regressors of the proposed model number 1 into Eq. 16 gives Eq. 17:

$$\begin{pmatrix} (CNg_1)^3 & (CNg_1)^2 & CNg_1 & (CTGT_1)^3 & (CTGT_1)^2 & CTGT_1 & (CWf_1)^3 & (CWf_1)^2 & CWf_1 & 1 \\ (CNg_2)^3 & (CNg_2)^2 & CNg_2 & (CTGT_2)^3 & (CTGT_2)^2 & CTGT_2 & (CWf_2)^3 & (CWf_2)^2 & CWf_2 & 1 \\ (CNg_3)^3 & (CNg_3)^2 & CNg_3 & (CTGT_3)^3 & (CTGT_3)^2 & CTGT_3 & (CWf_3)^3 & (CWf_3)^2 & CWf_3 & 1 \\ . & . & . & . & . & . & . & . & . & . \\ . & . & . & . & . & . & . & . & . & . \\ . & . & . & . & . & . & . & . & . & . \\ (CNg_{33})^3 & (CNg_{33})^2 & CNg_{33} & (CTGT_{33})^3 & (CTGT_{33})^2 & CTGT_{33} & (CWf_{33})^3 & (CWf_{33})^2 & CWf_{33} & 1 \\ (CNg_{34})^3 & (CNg_{34})^2 & CNg_{34} & (CTGT_{34})^3 & (CTGT_{34})^2 & CTGT_{34} & (CWf_{34})^3 & (CWf_{34})^2 & CWf_{34} & 1 \end{pmatrix} \times \begin{pmatrix} \alpha_1^1 \\ \alpha_2^1 \\ \alpha_3^1 \\ \alpha_4^1 \\ \alpha_5^1 \\ \alpha_6^1 \\ \alpha_7^1 \\ \alpha_8^1 \\ \alpha_9^1 \\ \alpha_0^1 \end{pmatrix} = \begin{pmatrix} CSHP_1 \\ CSHP_2 \\ CSHP_3 \\ . \\ . \\ . \\ CSHP_{33} \\ CSHP_{34} \end{pmatrix} \tag{17}$$

This system of equations is over-determined and does *not* have an exact solution. However, one can look for the 'closest' solution for this system, i.e. the 'best-fit' solution. This best-fit solution is denoted as $\{\hat{\alpha}\}$. The matrix constructed from $[A^T A]^{-1}A^T$ is the *projection matrix* which when multiplied by the vector b yields a solution in a subspace of A (Eq. 18). This solution serves as a best-fit or the closest solution one can determine.

$$\left\{\hat{\alpha}\right\}=\left[A^T A\right]^{-1}A^T\cdot\vec{b} \tag{18}$$

Following the above-described procedure one can immediately solve for the 10 coefficients of model number 1, see Eq. 19:

$$\left\{\alpha_i^1\right\}=\left[A^T A\right]^{-1}A^T\cdot\left\{CSHP\right\} \tag{19}$$

For the numerical set of flight-test data exemplified in this paper, model number 1 as given in Eq. 13 is presented as Eq. 20.

$$\left\{\alpha_i^1\right\}\triangleq\begin{pmatrix} \alpha_1^1 \\ \alpha_2^1 \\ \alpha_3^1 \\ \alpha_4^1 \\ \alpha_5^1 \\ \alpha_6^1 \\ \alpha_7^1 \\ \alpha_8^1 \\ \alpha_9^1 \\ \alpha_0^1 \end{pmatrix}=\begin{pmatrix} -0.0105 \\ 2.8486 \\ -250.48 \\ 2.386\times10^{-5} \\ -0.046874 \\ 30.406 \\ -8.556\times10^{-5} \\ 0.043963 \\ -5.6956 \\ 945.18 \end{pmatrix} \tag{20}$$

Similar procedure was repeated for all other 9 candidate models.

### C. Choosing the Right Model for the Task

Consider now the prediction errors of Model number 1 to 10 per an experimental data point as presented in Fig. 5 and calculated according to Eq. 21. For completeness Fig. 5 also includes data obtained from current analysis method presented in Figure 3. Looking at Fig. 5 one can see that, even before any statistical tool are to be involved, each proposed multivariable polynomial proposed by the MPOC method are performing better in predicting the engine output power as compared to the current method. However, one model needs to be chosen. Since a projection from a limited sample of experimental flight-test data to the entire population needs to be made, inferential statistics tools will be used. In general, a model is best replicating the experimental data if both the *mean* and *variance* of the estimation errors are zero. Obviously, this hypothetical perfect model is not to be found, however the following approach looks for the closest one.

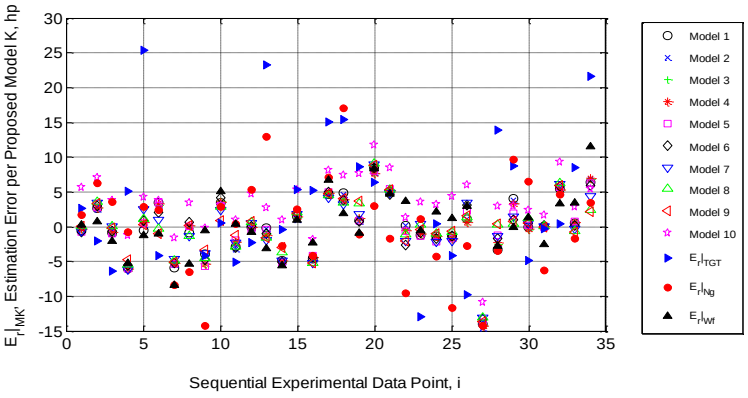


**Figure 5.** Estimation errors for the 10 proposed multivariable models & current single variable analysis. *The multivariable models performed far better in estimating the output power of the engine as compared with the experimental data.*

$$\vec{E}_r\Big|_{MK} = \left\{ CSHP_i - \left( CSHP_{MK} \right)_i \right\} \therefore i = 1,\ldots 34, k = 1,\ldots,10 \tag{21}$$

1) **The P-Value Approach**. The p-value approach was used to compare between the different 10 proposed models. The concept behind the *p-value* is thoroughly discussed in literature [Ref. 10]. The concept involves stating two contradicting hypothesis and use the experimental data to either support or reject the first hypothesis (the *Null Hypothesis*, $H_0$). In our analysis $H_0$ was set to claim that each of the multivariable models has an array of estimation errors with a zero *mean*. The level of significance for this statistical analysis was set at 1% (99% of confidence level). The p-values returned represent the *smallest* significant level that lead to rejecting the Null Hypothesis. In general, low p-values cast doubt on the validity of the Null Hypothesis and once submerge under the significance level of the test, the Null Hypothesis is rejected. All models except for model number 10 strongly supported the Null Hypothesis for the 1% significance level set. All first 5 models returned similar P-values, ranging from 0.999 to 1 with model number 2 being the only one to return

a computed P-value of 1. The P-value approach resulted therefore in the elimination of model number 10 from the list.

2) **Mean-Variance Plane**. A complementary approach to the P-value concept was to compare the models performance on the mean-variance plane. Figure 6 presents the paired values of mean and standard-deviation of the estimation prediction errors obtained for the first 9 proposed models.

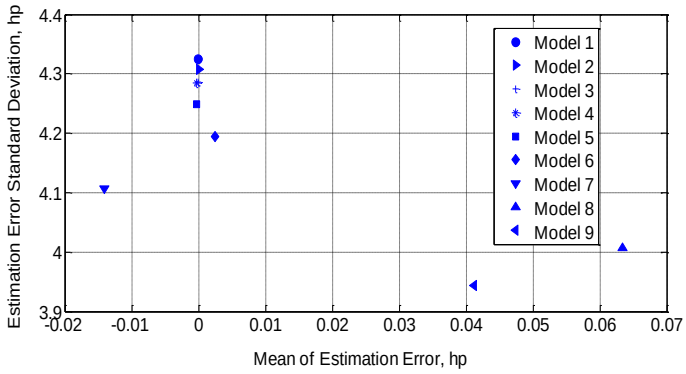


**Figure 6.** Various Models Performance on the Mean-Variance Plane. *Model number 6 start showing a divergence behavior in the mean of estimation error. Model number 10 was omitted from this figure due to an outstanding biased mean of estimation error (4hp).*

3) Based on the relative performance of all 10 models involved, model number 2 (Eq. 22 , 23) was chosen as the one to best represent the engine output power. Model number 2 will be further used to demonstrate the MPOC method.

$$CSHP_{M2} \approx \alpha_1^2 \left(CN_g\right)^3 + \alpha_2^2 \left(CN_g\right)^2 + \alpha_3^2 \left(CN_g\right) + \alpha_4^2 \left(CTGT\right)^3 + \alpha_5^2 \left(CTGT\right)^2 + \alpha_6^2 \left(CTGT\right) + \\ + \alpha_7^2 \left(CW_f\right)^3 + \alpha_8^2 \left(CW_f\right)^2 + \alpha_9^2 \left(CW_f\right) + \alpha_{10}^2 \left(CTGT\right)\left(CN_g\right) + \alpha_0^2 \tag{22}$$

$$\left\{\alpha_i^2\right\} \triangleq \begin{Bmatrix} \alpha_1^2 \\ \alpha_2^2 \\ \alpha_3^2 \\ \alpha_4^2 \\ \alpha_5^2 \\ \alpha_6^2 \\ \alpha_7^2 \\ \alpha_8^2 \\ \alpha_9^2 \\ \alpha_{10}^2 \\ \alpha_0^2 \end{Bmatrix} = \begin{Bmatrix} -0.0165 \\ 3.837 \\ -380.69 \\ 3.36\times10^{-5} \\ -0.075 \\ 41.809 \\ -8.35\times10^{-5} \\ 0.043 \\ -5.577 \\ 0.1486 \\ 2242.4 \end{Bmatrix} \tag{23}$$

**D. Estimation of the Maximum Output Power**

Once acquiring a multivariable polynomial to best describe the change in corrected engine output power based on other engine corrected parameters (compressor speed, temperature and fuel-flow), Model number 2 for the flight-test data of this paper, one can look for the maximum available output power of the engine under various atmospheric conditions. The engine output power will be limited by reaching one (or more) of its parameters. Finding the maximum output power is equivalent with finding an extremum point (maximum output power) under constraints (engine parameters: compressor speed, temperature or fuel flow). Finding an extremum point of a multivariable function under constraints is of a totally different nature from the case of extremum of a single parameter function. The most popular approach for the multivariable case is using Lagrange multipliers but this approach works with equalities constraints only whereas the problem we have in hand involves both equalities and inequalities constraints. One possible method for optimization under both equalities and inequalities constraints is the KKT (Karush-Kuhn-Tucker) method [Ref. 11]. Eq. 24 presents the general Lagrange equations required for satisfying extremum points of a multivariable function $f(x_i)$ subjected to 'm' number of inequalities constraints, $g(x_i)$, and 'l' number of equalities constraints $h(x_i)$. $\mu_j$ represent the Lagrange multipliers associated with the *inequalities* constraints and $\lambda_k$ represent the Lagrange multipliers associated with the *equalities* constraints.

$$\begin{aligned}
&\frac{\partial f}{\partial x_i}+\sum_{j=1}^{m}\left(\mu_j\frac{\partial g_j}{\partial x_i}\right)+\sum_{k=1}^{l}\left(\lambda_k\frac{\partial h_k}{\partial x_i}\right)=0\therefore i=1,2,3,...,n\\
&x=\left[x_1,x_2,...,x_n\right]\\
&g_j(x)\le 0\therefore\left(j=1,2,...,m\right)\\
&h_k(x)=0\therefore\left(k=1,2,...,l\right)
\end{aligned}\qquad(24)$$

The function to be maximized is model number 2 (Eq. 22, 23) subjected to several constraints. For this system of equations to be solvable, at least two *equality* constraints need to be provided. Those are fulfilled with the engine internal rule of operation, as explained hereinafter. Applying similar tools of the p-value and comparative evaluation on the mean-variance plane as described in section C above, a best fit surface was calculated to constitute the engine multivariable *internal rule of operation*. This surface which describes the relationship of the corrected engine temperature with both corrected compressor speed and corrected fuel-flow, complemented by the experimental data points is presented in Fig. 7. Based on this two constraints were selected.

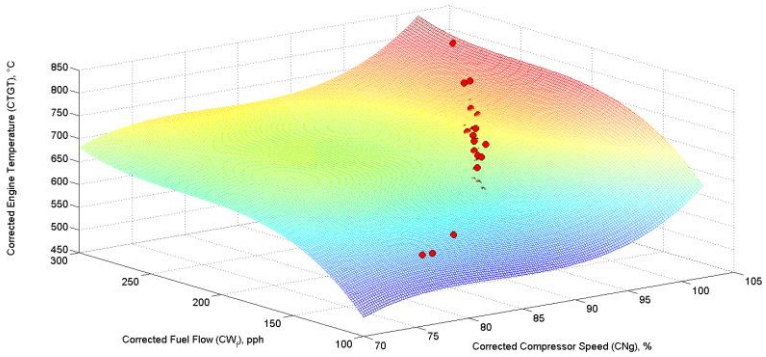


**Figure 7.** The engine multivariable internal rule of operation. *The relationship between the corrected engine temperature and the corrected values of the engine compressor speed and fuel flow. The circles presented are the experimental data points, which some are obscured by the best fit surface*.

The first one denoted as $h_1$ and presented in its implicit form in Eq. 25 relates between the corrected engine temperature and the corrected compressor speed. The second is denoted as $h_2$ and represents relationship between the corrected compressor speed and the corrected fuel-flow (Eq. 26). Note that $h_1$ and $h_2$ constraints are projections of the multivariable rule of operation onto two planes; the CTGT-CNg plane and the CNg-$CW_f$ plane respectively.

$$h_1 : CTGT - a_1\left(CNg\right)^3 - a_2\left(CNg\right)^2 - a_3\left(CNg\right) - a_4 = 0 \therefore \begin{pmatrix} a_1 \\ a_2 \\ a_3 \\ a_4 \end{pmatrix} = \begin{pmatrix} 0.0117 \\ -2.9739 \\ 258.49 \\ -7050 \end{pmatrix} \tag{25}$$

$$h_2 : CNg - b_1\left(CWf\right)^3 - b_2\left(CWf\right)^2 - b_3\left(CWf\right) - b_4 = 0 \therefore \begin{pmatrix} b_1 \\ b_2 \\ b_3 \\ b_4 \end{pmatrix} = \begin{pmatrix} 6.492\times10^{-6} \\ -0.00433 \\ 1.0621 \\ 2.9888 \end{pmatrix} \tag{26}$$

The *inequalities* constraint for the engine maximum output power are simply the operational limitations imposed on the engine. For the exemplary engine those are the continuous rating of the engine and are presented as Eq. 27, 28 and 29.

$$g_1 : CNg - \frac{105}{\sqrt{\theta}} \leq 0 \tag{27}$$

$$g_2 : CTGT - \frac{738}{\theta} \leq 0 \tag{28}$$

$$g_3 : CW_f - \frac{450}{\delta\sqrt{\theta}} \leq 0 \tag{29}$$

The partial differential equations based on Eq. 24 and the KKT conditions Eq. 27 to 29 for a *maximization* problem result in Eq. 30, 31 and 32.

$$\frac{\partial\left(CSHP_{M2}\right)}{\partial\left(CNg\right)} - \mu_1 + \lambda_1 \frac{\partial\left(h_1\right)}{\partial\left(CNg\right)} - \lambda_2 = 0 \tag{30}$$

$$\frac{\partial\left(CSHP_{M2}\right)}{\partial\left(CTGT\right)} - \mu_2 + \lambda_1 = 0 \tag{31}$$

$$\frac{\partial\left(CSHP_{M2}\right)}{\partial\left(CW_f\right)} - \mu_3 + \lambda_2 \frac{\partial\left(h_2\right)}{\partial\left(CWf\right)} = 0 \tag{32}$$

Eq. 30, 31 and 32 can be rearranged compactly as presented in Eq. 33.

$$\begin{pmatrix} \frac{\partial\left(CSHP_{M2}\right)}{\partial\left(CNg\right)} \\ \frac{\partial\left(CSHP_{M2}\right)}{\partial\left(CTGT\right)} \\ \frac{\partial\left(CSHP_{M2}\right)}{\partial\left(CW_f\right)} \end{pmatrix} = \begin{pmatrix} 1 & 0 & 0 & -\frac{\partial\left(h_1\right)}{\partial\left(CNg\right)} & -1 \\ 0 & 1 & 0 & -1 & 0 \\ 0 & 0 & 1 & 0 & -\frac{\partial\left(h_2\right)}{\partial\left(CW_f\right)} \end{pmatrix} \cdot \begin{pmatrix} \mu_1 \\ \mu_2 \\ \mu_3 \\ \lambda_1 \\ \lambda_2 \end{pmatrix} \tag{33}$$

The set of partial differential (Eq. 32) describes conditions for candidate engine corrected parameters representing maximization of the engine output power. This set does not have a unique solution but a solution with 2 degrees of freedom for the three different cases it represents. The first case (Case I) is when the compressor speed is at its maximum value, i.e., the engine output power is limited by the compressor speed. The second case (Case II) is when the output power is limited by the engine temperature and the last case (Case III) is a fuel-flow limited engine. Separating Eq. 33 into the three individual cases and applying the KKT conditions on the Lagrange multipliers associated with the inequalities constraints ($\mu_1$, $\mu_2$, $\mu_3$) eliminates the two degrees of freedom and makes each one of these cases to have a unique solution.

1) Case I – Compressor Speed Limited Engine.

Applying the KKT conditions for this case impose the following conditions on the Lagrange multipliers associated with the inequalities constraints (Eq. 34).

$$\{\mu_1 > 0, \mu_2 = 0, \mu_3 = 0\} \tag{34}$$

Combining Eq. 34 and Eq. 33 results in the following system of equations (Eq. 35):

$$\begin{pmatrix} \frac{\partial(CSHP_{M2})}{\partial(CNg)} \\ \frac{\partial(CSHP_{M2})}{\partial(CTGT)} \\ \frac{\partial(CSHP_{M2})}{\partial(CWf)} \end{pmatrix} = \begin{pmatrix} 1 & -\frac{\partial(h_1)}{\partial(CNg)} & -1 \\ 0 & -1 & 0 \\ 0 & 0 & -\frac{\partial(h_2)}{\partial(CWf)} \end{pmatrix} \cdot \begin{pmatrix} \mu_1 \\ \lambda_1 \\ \lambda_2 \end{pmatrix} \therefore \begin{Bmatrix} \mu_1 > 0 \\ CNg = \frac{105}{\sqrt{\theta}} \\ CTGT < \frac{738}{\theta} \\ CWf < \frac{450}{\delta\sqrt{\theta}} \end{Bmatrix} \tag{35}$$

2) Case II – Temperature Limited Engine.

Applying the KKT conditions for this case impose the following conditions on the Lagrange multipliers associated with the inequalities constraints (Eq. 36).

$$\{\mu_1 = 0, \mu_2 > 0, \mu_3 = 0\} \tag{36}$$

Substituting Eq. 36 into Eq. 33 results in the following set of equations (Eq. 37):

$$\begin{pmatrix} \frac{\partial(CSHP_{M2})}{\partial(CNg)} \\ \frac{\partial(CSHP_{M2})}{\partial(CTGT)} \\ \frac{\partial(CSHP_{M2})}{\partial(CWf)} \end{pmatrix} = \begin{pmatrix} 0 & -\frac{\partial(h_1)}{\partial(CNg)} & -1 \\ 1 & -1 & 0 \\ 0 & 0 & -\frac{\partial(h_2)}{\partial(CWf)} \end{pmatrix} \cdot \begin{pmatrix} \mu_2 \\ \lambda_1 \\ \lambda_2 \end{pmatrix} \therefore \begin{Bmatrix} \mu_2 > 0 \\ CNg < \frac{105}{\sqrt{\theta}} \\ CTGT = \frac{738}{\theta} \\ CWf < \frac{450}{\delta\sqrt{\theta}} \end{Bmatrix} \tag{37}$$

3) Case III – Fuel-Flow Limited Engine.

Finally the third case is when the maximum output power of the engine is bounded by reaching the maximum fuel-flow the pump is capable of delivering to the engine. Applying the KKT conditions for this case impose the following conditions on the Lagrange multipliers associated with the inequalities constraints (Eq. 38).

$$\{\mu_1 = 0, \mu_2 = 0, \mu_3 > 0\} \tag{38}$$

Combining Eq. 38 with Eq. 33 results in the following set of equations (Eq. 39):

$$\begin{pmatrix} \frac{\partial(CSHP_{M2})}{\partial(CNg)} \\ \frac{\partial(CSHP_{M2})}{\partial(CTGT)} \\ \frac{\partial(CSHP_{M2})}{\partial(CWf)} \end{pmatrix} = \begin{pmatrix} 0 & -\frac{\partial(h_1)}{\partial(CNg)} & -1 \\ 0 & -1 & 0 \\ 1 & 0 & -\frac{\partial(h_2)}{\partial(CWf)} \end{pmatrix} \cdot \begin{pmatrix} \mu_3 \\ \lambda_1 \\ \lambda_2 \end{pmatrix} \therefore \begin{Bmatrix} \mu_3 > 0 \\ CNg < \frac{105}{\sqrt{\theta}} \\ CTGT < \frac{738}{\theta} \\ CWf = \frac{450}{\delta\sqrt{\theta}} \end{Bmatrix} \tag{39}$$

The next section demonstrates the specifics of Case II using the exemplary flight-test data. Similar methodology can be applied to find the maximum output power for the other two cases.

The set of equations specified in Eq. 37 has a solution if and only if the rank of the system matrix equals the rank of the auxiliary matrix. This solution is also unique if both ranks equal three (the three Lagrange multipliers). This requirement for a unique solution can be stated mathematically as in Eq. 40.

$$rank\begin{pmatrix} 0 & -\frac{\partial(h_1)}{\partial(CNg)} & -1 \\ 1 & -1 & 0 \\ 0 & 0 & -\frac{\partial(h_2)}{\partial(CWf)} \end{pmatrix} = rank\begin{pmatrix} 0 & -\frac{\partial(h_1)}{\partial(CNg)} & -1 & \frac{\partial(CSHP_{M2})}{\partial(CNg)} \\ 1 & -1 & 0 & \frac{\partial(CSHP_{M2})}{\partial(CTGT)} \\ 0 & 0 & -\frac{\partial(h_2)}{\partial(CWf)} & \frac{\partial(CSHP_{M2})}{\partial(CWf)} \end{pmatrix} = 3 \tag{40}$$

Instead of searching for a pair of corrected compressor speed and corrected fuel-flow under a limited corrected temperature ($CTGT_{limit}$) to satisfy Eq. 37, one can simplify the process by using a "back-door" approach: for each and every combination of atmospheric conditions a pair of candidate corrected compressor speed and corrected fuel flow will be suggested provided via the engine internal rule of operation (Eq. 25 and 26). These candidate pairs complemented with the engine temperature limit will then be evaluated for fulfillment of the KKT conditions required for maximization of the engine output power. Since the equations specified in Eq. 37 have a unique solution they can be rearranged as in Eq. 41. The three engine parameters (candidates for maximum output power) can be used in Eq. 41 to solve for the Lagrange multipliers. The three candidate simultaneous engine parameters will be proved valid to define a maximum output power of a temperature limited engine if and only if the solution of the system specified as Eq. 41 is achieved while coinciding with the KKT conditions required for the case.

$$\begin{pmatrix} \mu_2 \\ \lambda_1 \\ \lambda_2 \end{pmatrix} = \begin{pmatrix} \dfrac{-1}{\left(\partial h_1/\partial CNg\right)} & 1 & \dfrac{1}{\left(\partial h_1/\partial CNg\right)\left(\partial h_2/\partial CW_f\right)} \\ \dfrac{-1}{\left(\partial h_1/\partial CNg\right)} & 0 & \dfrac{1}{\left(\partial h_1/\partial CNg\right)\left(\partial h_2/\partial CW_f\right)} \\ 0 & 0 & \dfrac{-1}{\left(\partial h_2/\partial CW_f\right)} \end{pmatrix} \cdot \begin{pmatrix} \dfrac{\partial\left(CSHP_{M2}\right)}{\partial\left(CNg\right)} \\ \dfrac{\partial\left(CSHP_{M2}\right)}{\partial\left(CTGT\right)} \\ \dfrac{\partial\left(CSHP_{M2}\right)}{\partial\left(CWf\right)} \end{pmatrix} \therefore KKT: \begin{Bmatrix} \mu_2 > 0 \\ CNg < \dfrac{105}{\sqrt{\theta}} \\ CTGT = \dfrac{738}{\theta} \\ CWf < \dfrac{450}{\delta\sqrt{\theta}} \end{Bmatrix} \quad (41)$$

This procedure was carried out using the engine internal rules of operation (Eq. 25 and 26) for different day conditions (ISA, ISA+10°C, ISA+20°C, ISA-5°C & ISA-10°C). Figure 8 presents the maximum output power of the exemplary engine along with all KKT requirements as a function of pressure-altitude for an ISA day conditions. It can be seen that

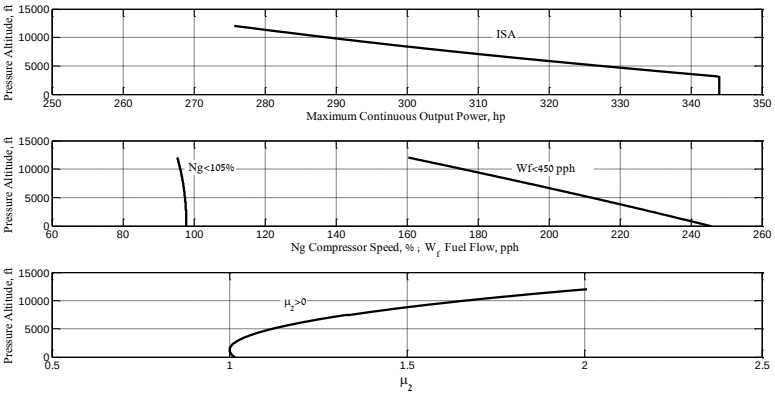


**Figure 8.** A simultaneously presentation of all engine parameters for pressure-altitude between sea level and 12,000 ft. under standard day conditions (ISA). The engine is temperature limited at 738°C. *Note the fulfillment of all KKT conditions for output power maximization of the temperature limited engine.*

all the KKT conditions are met. Figure 9 presents the maximum continuous output power of the engine as a function of pressure-altitude for different day conditions. The maximum continuous output power of the engine is temperature limited under all atmospheric conditions presented in Fig. 9. Note the KKT requirements were omitted from Fig. 9 although they were all met.

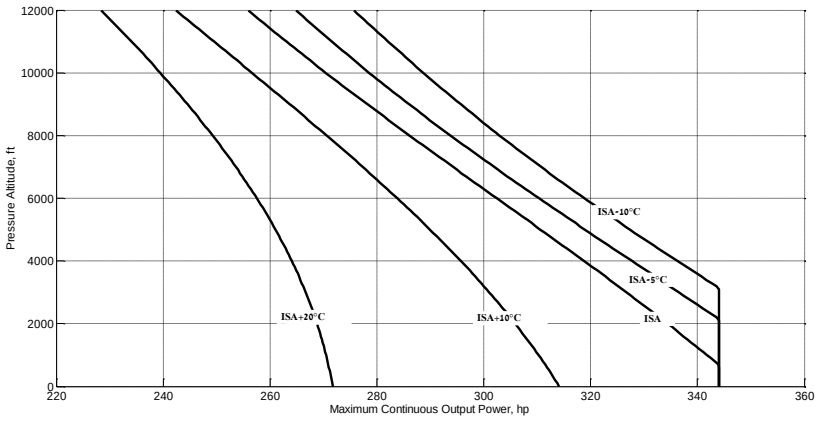


**Figure 9.** Estimation of the engine maximum continuous output power between sea level to 12,000 ft. under different day conditions. *The maximum continuous power of the engine was estimated to be temperature limited. Note the engine maximum continuous power for ambient temperatures of a standard day profile (ISA) and below is bounded by the helicopter transmission rating.*

## E. Comparison of Maximum Output Power for Current and MPOC method

Finally, the estimated maximum engine output power was compared using both the current and the proposed MPOC methods. This comparison is presented in Fig. 12. Looking at this figure one can see that both methods demonstrated similar results for atmospheric conditions close to those prevailed during the actual flight-tests (ISA+21°C); however, while the current single-variable method completely collapsed under ISA and colder day conditions, the MPOC method predicted reasonable and logical estimations for ISA and colder day conditions.

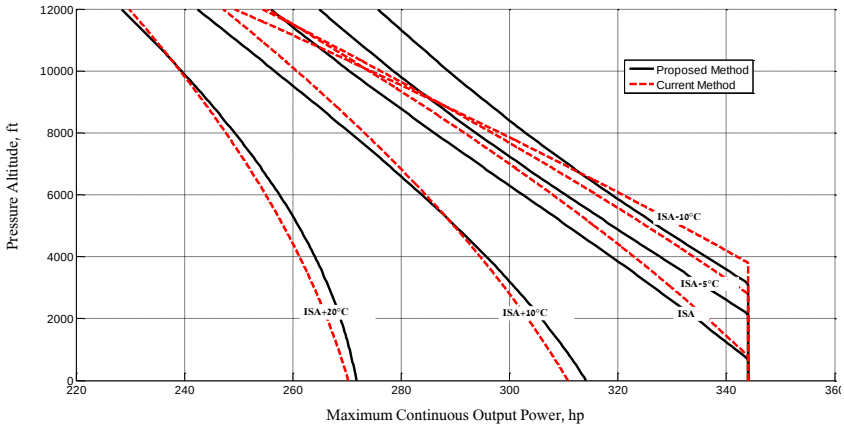


**Figure 10.** Comparison between the proposed and the current methods. *It can clearly be seen that while the current single variable method collapses under the estimation for maximum continuous output power for standard day conditions and colder, the proposed multivariable method still provides a logical estimation.*

## IV. Conclusions

The output power of a helicopter gas turbine engine is a multivariable problem that can be non-dimensionalized as any other physically meaning problem. Over simplification of the problem as linear combination of single-variable models does *not* provide sufficient accuracy and frequently provides unrealistic estimations for maximum output power under atmospheric conditions different than those prevailed during the test. The novel method presented in this paper (Multivariable Polynomial Optimization under Constraints, MPOC) is based on *multivariable* polynomials which proved substantial better performance in estimating the output power of a BO105 helicopter used as example in this paper (over 300% of improvement). The P-value concept complemented with a comparative performance on the mean-variance plane were used successfully as an inferential statistical tool for sorting between various candidate multivariable models to represent the gas turbine engine output power. Predicting the maximum output power of the engine can be regarded, mathematically, as an optimization problem of a multivariable function subjected to both equalities and inequalities constraints. The equalities constraints were based on the experimental data and the inequalities were provided by the engine operating limitations. While the current method provided unrealistic results for certain atmospheric conditions, the proposed MPOC method demonstrated adequate prediction performance for a wider range of atmospheric conditions. Although the current single-variable method is simple to use it should be utilized only as a first estimation and not as a formal analysis tool in the process of estimating the maximum output power of a gas turbine engine. The approach presented in this paper will be expanded in the future to include flight-test data of other types of helicopters and engines. Future research can also include a comparative analysis between a broader base of candidate multivariable polynomials in order to better understand which type of regressors are performing better in modeling the output power of a gas turbine engine and the reason for that.

## References


[1] Advisory Group for Aerospace Research & Development (AGARD), *Flight Test Techniques Series.* AGARD-AG-300, 1995

[2] Cooke, A.K. and Fitzpatrick EWH, *Helicopter Test and Evaluation*, 1st ed., AIAA Education Series, 2002

[3] Knowles, P. *The Application of Non-dimensional Methods to the Planning of Helicopter Performane Flight Trials and Analysis Results,* Aeronautical Research Council ARC CP 927, 1967

[4] Buckingham, E., "On Physically Similar Systems; Illustrations of the Use of Dimensional Equations," *Physical Review*, Vol. IV, No. 4, 1914, pp. 345, 376, doi: 10.1103/PhysRev.4.345

[5] National Test Pilot School, *Professional Course Textbook Series, Vol. VII, Rotary Wing Performance Flight Testing,* Mojave, 2017, Chap. 5.

[6] Ulbrich, N., Regression Model Optimization for the Analysis of Experimental Data, AIAA 2009–1344, paper presented at the 47th AIAA Aerospace Sciences Meeting and Exhibit, Orlando, Florida, January 2009

[7] Ulbrich, N., Optimization of Regression Models of Experimental Data using Confirmation Points, AIAA 2010–930, paper presented at the 48th AIAA Aerospace Sciences Meeting and Exhibit, Orlando, Florida, January 2010

[8] Zhao, D. and Xue, D., A multi-surrogate approximation method for metamodeling, *Engineering with Computers,* Vol. 27, No. 2, pp. 139-153, 2011.

[9] Strang, G., *Introduction to Linear Algebra*, 5th ed., Wellesley-Cambridge Press, Wellesley MA, 2016, Chap. 4.

[10] Guttman, I., Wilks, S., and Hunter, J., *Introductory Engineering Statistics*, 2nd ed., John Wiley & Sons, Inc., New York, 1971, Chap. 10.

[11] Singiresu, R., *Engineering Optimization Theory and Practice*, 4th ed., John Wiley & Sons, Inc., New Jersey, 2009, Chap. 2.